A Modular Tool Chain for High Performance CFD Simulations in Intracranial Aneurysms

Georg Mach*, René Heinzl*, Philipp Schwaha†, Franz Stimpfl*, Josef Weinbub*, Siegfried Selberherr* and Camillo Sherif**

*Institute for Microelectronics, Technische Universität Wien, Gußhausstraße 27-29, 1040 Vienna, Austria
†Shenteq s.r.o, Záhradnícka 7, 811 07 Bratislava, Slovak Republic
**Abteilung für Neurochirurgie, KH Rudolfstiftung Wien, Juchgasse 25, 1030 Vienna, Austria

Abstract. We present a modular tool chain for high performance CFD simulations of pulsatile blood flow in intracranial aneurysms. We describe a path from in-situ imaging (ie. CT and MRI) to flow simulations and show different modules for obtaining anatomically accurate and allover smooth meshes suitable for computed fluid dynamics (CFD) as well as methods for computing the blood flow in a robust and high performing way.

Keywords: high performance CFD, flow simulation, image segmentation, adaptive meshing, hp-refining, parallelization, DG-FEM
PACS: 07.05.Rm, 07.05.Tp, 87.19.U-,89.20.Ff

INTRODUCTION

Intracranial aneurysms occur in about $1-5\%$ of the adult population and about $20-50\%$ of these rupture during their lifetime [1]. The mortality due to hemmorage following a rupture is between $40-50\%$. Surgical treatment of cerebral aneurysms according to gold standard procedures is associated with a post- and intraoperative mortality between $0.5-1.5\%$ [2]. Due to the considerable risks involved, careful analysis of the aneurysm is warranted when evaluating surgery. Here we propose non invasive means such as imaging and numerical intraaneurysmal flow studies.

Contrary to the benefits awarded by the rapid developments of resolution and accuracy of diagnostic imaging techniques, the new possibilities of visualization and simulation have not yet found their way into clinical practice. Due to the increasing computational power of both CPUs and GPUs three-dimensional visualization and CFD simulations are no longer the prerogative of supercomputers.

We present a modular tool chain suitable for modern desktop computers and so for clinical, daily routine. Figure 1 depicts the sequence to get from imaging to a flow simulation. The main steps are segmentation, meshing, and the proper selection of simulation parameters as well as simulation methods. The goal is to get an accurate and fast simulation of the pulsatile blood flow in a vessel system.

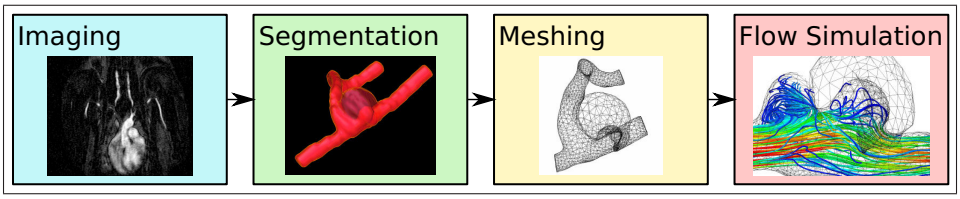

FIGURE 1. The sequence from imaging to flow simulation.

On the way from imaging to blood flow simulations the following characteristics are crucial and have been achieved by our tool chain:

- modularity, compatibility, and extensibility for easily exchanging and adding components, which is generally important due to ongoing enhancements on all parts of the tool chain.
- usability and high performance are essential criteria for clinical practice. Not only the time spent waiting for results of a simulation but also the time to get familiar with the software are strictly limited.
- accuracy and robustness for a wide range of applications and solving even mathematically ill-conditioned cases.

CP1281, *ICNAAM, Numerical Analysis and Applied Mathematics, International Conference 2010*
edited by T. E. Simos, G. Psihoyios, and Ch. Tsitouras

THE TOOL CHAIN

In this section we explain the single parts of the tool chain. The characteristics and requirements of the individual modules of the tool chain, which are formed by selected specialized applications, are discussed and their contribution to the aforementioned aims is shown.

The first step after imaging itself is to segment the input data set in order to make it accessible to the subsequent steps. A three-dimensional structure has to be extracted from a series of two-dimensional gray value images which represent slices through the area of interest. The extraction of structures follows the boundaries between different tissues [3]. Segmentation makes use of and relies on contrast as well as on geometrical factors encountered. The experience and expertise of a user are essential, as all subsequent steps depend on ensuring adequate results in this step.

Two different software packages have been used in the segmentation module, `VMTK` [4] and `ITK-Snap` [5], both providing multiple segmentation algorithms but differing in their abilities of post processing and the usability. `ITK-Snap` focuses on usability and provides a graphical interface during the whole process. `VMTK`, on the other hand, whose components have to be controlled by alternating between command line and GUI, provides methods for smoothing and a feature for a skeletonization to center lines and rebuilding of the structure with circles of average diameter [6]. For smoothing and cropping of the extracted structures, `MeshLab` [7] has been used. All of the tools support several input and output file formats, so a high degree of modularity and compatibility is achieved.

After segmentation and post processing the resulting structure has to be meshed, the model has to be specified as a mathematical problem, and the respective equations have to be solved. To achieve the highest possible grade of modularity an extended version of a generic mesh generator interface [8, 9] has been used, allowing generic access to various mesh generators [10–12].

In the current configuration we chose a suite with meshing and solving software, `NetGen` [12] as mesher and `NGSolve` [13] in conjunction with the `NGSFlow`-package [14], providing adaptive meshing with hp-refinement as well as a high performance and robust way of solution.

Contrary to uniform refinement which results in many unnecessarily fine regions and therefore excessively long simulation times, adaptive meshing contributes to the necessity of inhomogeneous and anisotropic refinement [15]. The hp-adaptivity provides different ways to refine an element, which are preferable to from both h- and p-adaptivity due to the large number of combinations for the polynomial degrees on the subelements. The hp-refinement combines adaptively elements with variable size h and polynomial degree p in order to achieve exponential convergence rates [16].

No matter how sophisticated the deployed refinement strategies are, they increase the computational burden of the simulation. Therefore, it is necessary to make efficient use of the available computing recourses. The recent introduction of multi core machines into the main stream makes parallelization a highly interesting goal, even for desktop systems. Beside deploying parallel matrix solvers [17, 18] for the solution of the equation system, assembly is a promising candidate for parallelization in the FEM procedure. This can be facilitated by partitioning the set of traversed elements into disjoint parts [19].

The mathematical problem to solve in this case is described by the incompressible, unsteady Navier-Stokes equations [20], which are nonlinear partial differential equations. They are obtained when considering incompressible flow of Newtonian fluids. In our tool chain the local discretization is performed by the Discontinuous Galerkin Finite Element Method (DG-FEM) [21], which combines features of the finite element (higher order approximations) and the finite volume (flow conservation) methods [22]. For time discretization the chosen modules use implicit-explicit (IMEX) schemes [23]. This method combines both robustness and high performance by avoiding to solve nonlinear, non symmetric equations as well as to integrate the stiff part with an explicit scheme.

APPLICATION OF THE TOOLCHAIN

The application we present is a model of an experimental aneurysm created on an artificial bifurcation of the carotis communis of a rabbit [24]. Due to intracranial aneurysms are mostly diagnosed by chance the experimental aneurysms provide accurate models with the possibility of miscellaneous adjustments regarding size, position an other geometrical parameters. The diagnostic imaging was performed with an $1.5T$ MRT, where several sequences of DICOM images were taken each pre and post contrast enhancement. The aneurysm we modeled was embolized and then partially recanalized.

After segmenting the area of interest with `ITK-Snap` and `MeshLab`, the meshing was performed with `NetGen`, as outlined in the previous section. Subsequently, we solved the non-stationary, incompressible Navier-Stokes equations as described for the flow simulation module. Figure 2 shows the segmented aneurysm as well as the resulting mesh which is used as input for the simulation.

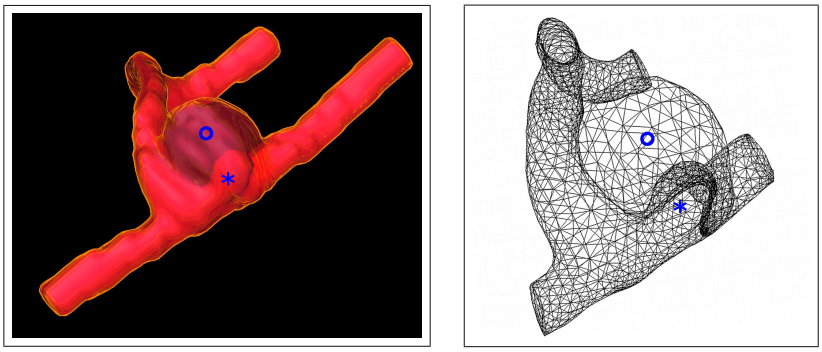

FIGURE 2. Segmented and meshed aneurysm. The embolized sack ($\circ$) as well as the recanalized part ($*$) are shown.

For the boundary conditions we assumed the vessel walls to be non porous, the outlets to be open, and the inlet to carry a pulsatile flow with $60\frac{beats}{min}$. The periodic time dependent flow profile is depicted in Figure 3. It is applied in the center where it has a minimum velocity $v_{min} = 460\frac{mm}{s}$ and a maximum velocity $v_{max} = 910\frac{mm}{s}$ perpendicular to the inlet plane. From there it decays quadratically to meet the no slip boundary conditions.

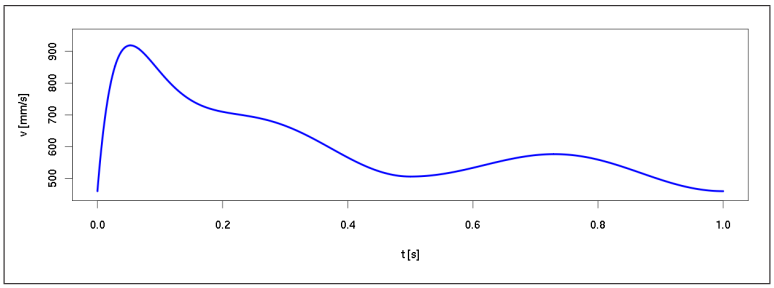

FIGURE 3. The time dependent flow profile for the inlet was recovered from Doppler-sonography.

Because of the small vessel diameters and the comparatively high velocities the non-rigidity of the vessel walls was neglected and the blood was modeled as Newtonian fluid with a density $\rho = 1.055 \cdot 10^{-6}\frac{kg}{mm^3}$ and a dynamic viscosity $\eta = 4.9 \cdot 10^{-6}\frac{kg}{mm \cdot s}$, from which a kinematic viscosity $\nu = 4.645\frac{mm^2}{s}$ was derived. Both, the boundary conditions and the blood flow parameters (except the time dependent profile), were taken from literature [25].

The streamlines of the velocity vector field in Figure 4 represent the resulting blood flow in the aneurysm, depicting a parabolic flow profile with its maximum at the centerline of the vessel. The figure shows how a turbulence is caused by the flow in the recanalized part which results in higher shear stress and therefor higher risk of rupture. The rest of the aneurysm sack has no flow, since it has been embolized.

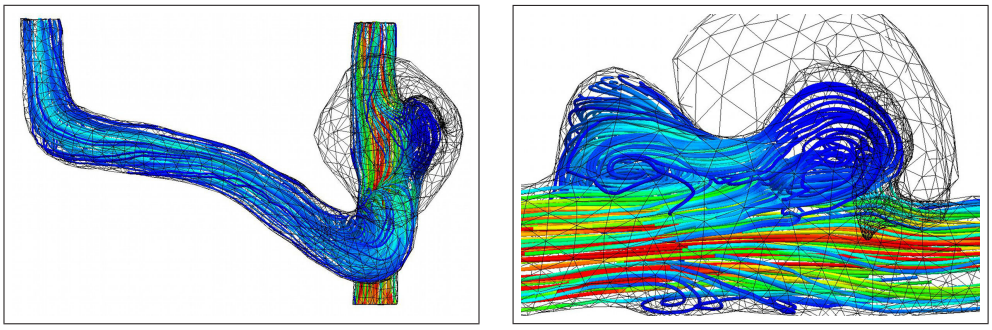

FIGURE 4. Velocity of the blood flow (from blue to red implying slower to faster). **Left:** Flow through the parent vessels and the recanalized part. The embolized part of the aneurysm sack has no flow. **Right:** Turbulences caused by the recanalized part.

CONCLUSION AND OUTLOOK

We presented a modular tool chain for high performance CFD simulations in intracranial aneurysms. The focus was on modularity and high performance, but also on robustness, usability and compatibility. The application was demonstrated on an experimental aneurysm at an artificial bifurcation of the carotis.

Further investigations on usability and automatization have to be done. So far most parts regarding segmentation depend on the user's skills and can not be fully automated. Artificial intelligence in combination with anatomic atlases [26] could be a possible improvement. Also a graphical input for the boundary conditions would be helpful to use the tool chain in clinical practice.

ACKNOWLEDGMENTS

We would like to thank the main developers of `NGSFlow`, Joachim Schöberl and Christoph Lehrenfeld, for maintaining, extending, and bug fixing the package on very short notice. We are grateful for the sonographic images the Tierklinik Hollabrunn provided us with. Special thanks to Florian Gerstl for proofreading. This work has been supported by the Austrian Science Fund FWF, project P19532-N13.

REFERENCES

1. J. Brisman, J. Song, and D. Newell, "Cerebral Aneurysms," in *The New England Journal of Medicine*, Massachusetts Medical Society, USA, 2006, vol. 355, pp. 928–939, ISSN 1533-4406.
2. R. Fogelholm, J. Hernesniemi, and M. Vapalahti, "Impact of early surgery on outcome after aneurysmal subarachnoid hemorrhage," in *Stroke*, American Stroke Association, USA, 1993, vol. 24, pp. 1649–1654, ISSN 1524-4628.
3. S. Acton, and N. Ray, *Biomedical Image Analysis: Segmentation*, Morgan & Claypool, Austin, 2009, ISBN 9781598290219.
4. Vascular Modeling Toolkit (VMTK) (2009), URL `http://www.vmtk.org`.
5. ITK-Snap (2009), URL `http://www.itksnap.org`.
6. L. Antiga, *Patient-Specific Modeling of Geometry and Blood Flow in Large Arteries*, Ph.D. thesis, Politecnico di Milano (2002).
7. MeshLab (2010), URL `http://meshlab.sourceforge.net`.
8. J. Weinbub, *Adaptive Mesh Generation*, Master's thesis, Technische Universität Wien (2009).
9. F. Stimpfl, J. Weinbub, R. Heinzl, P. Schwaha, and S. Selberherr, "A Unified Topological Layer for Finite Element Space Discretization," in *Proceedings International Conference of Numerical Analysis and Applied Mathematics, submitted*, 2010.
10. Triangle (2005), URL `http://www.cs.cmu.edu/~quake/triangle.html`.
11. Tetgen (2009), URL `http://tetgen.berlios.de`.
12. NetGen (2010), URL `http://sourceforge.net/projects/netgen-mesher`.
13. NGSolve (2010), URL `http://sourceforge.net/projects/ngsolve`.
14. NGSFlow (2010), URL `http://sourceforge.net/projects/ngsflow`.
15. T. Plewa, *Adaptive Mesh Refinement - Theory and Applications*, Springer, Berlin, 2005, ISBN 3-540-21147-0.
16. I. Babuska, and M. Suri, "The P and H-P Versions of the Finite Element Method, Basic Principles and Properties," in *SIAM Review*, Society for Industrial and Applied Mathematics, USA, 1994, vol. 36, pp. 578–632, ISSN 0036-1445.
17. Portable, Extensible Toolkit for Scientific Computation (PETSc) (2010), URL `http://www.mcs.anl.gov/petsc`.
18. Trilinos (2010), URL `http://trilinos.sandia.gov`.
19. R. Heinzl, *Concepts for Scientific Computing*, Ph.D. thesis, Technische Universität Wien (2007).
20. D. Acheson, *Elementary Fluid Dynamics*, Clarendon Pr., Oxford, 1992, ISBN 0-19-859660-X.
21. D. Schötzau, C. Schwab, and A. Toselli, "Mixed hp-DGFEM for incompressible flows," in *Research report Seminar für Angewandte Mathematik*, Eidgenössische Technische Hochschule Zürich, 2002, vol. 2002-10.
22. D. Arnold, F. Brezzi, B. Cockburn, and L. Marini, "Unified Analysis of Discontinuous Galerkin Methods for Elliptic Problems," in *SIAM Journal of Numerical Analysis*, Society for Industrial and Applied Mathematics, USA, 2002, vol. 39, pp. 1749–1779, ISSN 1095-7170.
23. C. Lehrenfeld, *Hybrid Discontinuous Galerkin Methods for Solving Incompressible Flow Problems*, Master's thesis, Rheinisch-Westfälische Technische Hochschule Aachen (2010).
24. M. Forest, and G. O'Reilly, "Production of experimental aneurysms at a surgically created arterial bifurcation," in *American Journal of Neuroradiology*, American Society of Neuroradiology, USA, 1989, vol. 10, pp. 400–402, ISSN 1936-959X.
25. T. Ohshima, S. Miyachi, K. Hattori, I. Takahashi, K. Ishii, T. Izumi, and J. Yoshida, "Risk of Aneurysmal Rupture: the Importance of Neck Orifice Positioning-Assessment Using Computational Flow Simulation," in *Neurosurgery*, Lippincott Williams & Wilkins, USA, 2008, vol. 62, pp. 767–775, ISSN 1524-4040.
26. C. Ciofolo, and C. Barillot, "Atlas-based segmentation of 3D cerebral structures with competitive level sets and fuzzy control," in *Medical Image Analysis*, Elsevier, Netherlands, 2009, vol. 13, pp. 456–470, ISSN 1361-8415.